04-82-70

METALLOGRAPHY 15:43–52 (1982)

Welding Structures in Gas Tungsten Arc-Welded Zircaloy-4

TERESA ESTELA PEREZ AND MARÍA EUGENIA SAGGESE

Instituto de Ensayos no Destructivos (INEND), Comision Nacional de Energia Atomica, Avenida del Libertador 8250, 1429, Buenos Aires, Argentina

Microstructures were obtained by the gas tungsten arc welding of tubes to end caps in Zircaloy-4 fuel elements and analyzed metallographically. This article characterizes the structures and the relationships between the operative variables and structural elements and properties. The final joint properties are shown to be greatly influenced by the different structural elements, including microstructure, porosity, and inclusions. The secondary structure found after welding is Widmanstätten, varying from a parallel-plate to a basketweave pattern. Welding thermal cycles are inherently inhomogeneous, affecting both plate width and β primary grain.

Introduction

Because of the influence of the weldments on the service performance of welded structures, their analysis assumes fundamental importance. It is known that the welding process determines the presence, size, distribution, and morphology of the structural elements, including macro- and microsegregation, microstructure (phase morphology), inclusions, porosity, and precipitates. This article characterizes the microstructures resulting from gas tungsten arc welding (GTAW) of Zircaloy-4.

The microstructures that can be present in Zircaloy-4 have been studied by several authors. Woo and Tangri [1] correlate the oxygen content and cooling rate with the microstructure of β-quenched Zircaloy-4 alloys. They identify the following secondary structures:

lenticular α (Lα): coarse, platelike structures with irregular and jagged boundaries formed by slow cooling;
parallel plate α (Wppα): Widmanstätten α structures formed on one habit plane of preexisting β;
basketweave α (Wbα): nonparallel structures of Widmanstätten α re-

© Elsevier North Holland, Inc., 1982
52 Vanderbilt Ave., New York, NY 10017

0026-0800/82/010043 + 10$02.75

sulting from the random precipitation of α plates on a number of planes in one β grain; and

martensite α′ (Mα′): needlelike structures similar in appearance and mode of formation to ferrous martensites and formed by diffusionless transformation.

With increasing cooling rate the structures change in the order

$$L\alpha \rightarrow W\alpha \rightarrow M\alpha';$$

at the same time, the plate width decreases. Increasing the oxygen content at a fixed cooling rate enhances the diffusion-controlled transformation as

$$L\alpha \leftarrow W\alpha \leftarrow M\alpha',$$

and the plate width is also increased.

Ökvist and Källström [2] discuss the influence of the carbon content and conclude that it is important in determining the type of Widmanstätten structure that will appear for a fixed cooling rate. They associate the presence of Wbα with a relatively high carbon content (100–200 ppm). On the other hand, for a low carbon content (<50 ppm) the structure will be Wppα. In the first case microscopy revealed 5×10^8 cm^{-3} particles of diameter >0.4 μm as nucleation sites for the α-phase parallel-plate structure. Microprobe analysis revealed carbon in these particles. Electron diffraction patterns of extraction replicas showed the particles to be fcc with a lattice parameter of about 4.7 Å. X-ray diffraction of the particles convincingly proved the presence of zirconium carbide with lattice parameter 4.68 Å. The effect of zirconium carbide in causing a basketweave structure was confirmed in the full-scale production of Zircaloy by the addition of carbon to a melt of low-carbon zirconium sponge.

Holt [3] observed two Widmanstätten morphologies differing only in carbon content (153 vs 58 ppm) in nominally similar Zircaloy-4. As the carbon increases, the resultant structure is Wbα, in accord with the observation of Ökvist and Källström. This difference in structure coincides with a difference in the kinetics of the β → α phase transformation. Holt considers that this difference in kinetics is the result of different nucleation rather than growth mechanisms. This is related to the abundance and size of second-phase particles insoluble in the β phase, which act as nucleation sites in preference to the β-grain boundaries. Holt finds evidence that some of the particles are NaCl cubic structures with a lattice parameter of 5.25 Å, which corresponds to zirconium phosphide. He also suggests that the presence of suitable nucleation sites may depend not only on the carbon content but also on the oxygen, nitrogen, and phosphorus present.

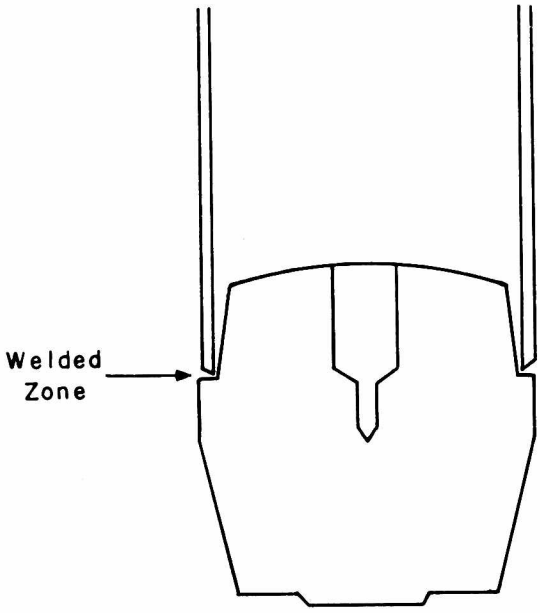

FIG. 1. Schematic diagram of the welding position.

Metallography

The samples analyzed were weldments of end caps to tubes in fuel elements. Figure 1 shows the position of the weld. Metallographic observations were performed on a longitudinal cross-section.

The specimens were mounted in epoxy resin, polished with 600 paper (CSi), and then chemically polished with a solution of 3% HF, 47% HNO_3, and 50% H_2O to reveal the structure. The micrographs were obtained in the optical microscope MeF Reichert, with either polarized or normal light. The scanning electron microscope was also used.

Results

The tubes have a textured structure, due to the fabrication processes (Fig. 2). The Zircaloy-4 bars from which the end caps are machined usually display porosity aligned along the centerline. To eliminate this alignment and to conform with welding specifications, the end caps are heated (prior to welding) with a GTAW torch until the surface is molten.

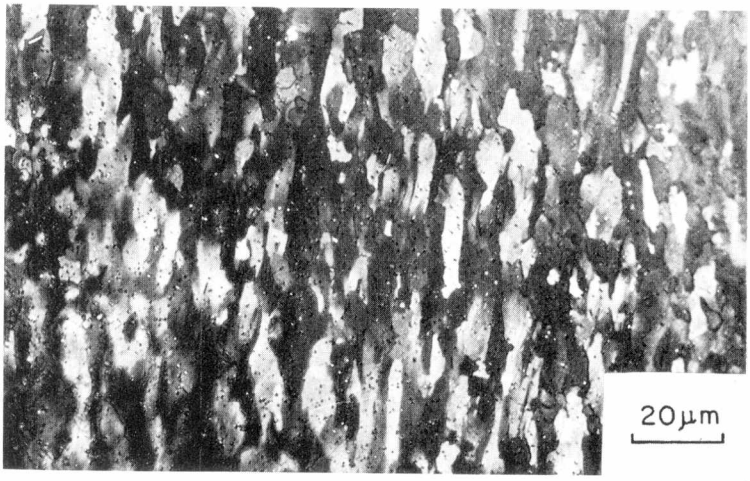

FIG. 2. Optical micrograph of the tube structure (taken in polarized light).

The equiaxed α structure [Figs. 3(a) and 3(a′)] is then modified in a fixed sequence: Figures 3(b) and 3(b′) illustrate the transition zone between a needlelike martensitic (Mα′) colony structure and a fine basketweave α structure (Wbα), and the micrographs in Figs. 3(c) and 3(c′) show the ensuing predominantly Wbα structure containing a certain proportion of parallel plate α (Wppα).

This structure can be observed in more detail using the scanning electron microscope [Figs. 4(a) and 4(b)], which allows higher magnification with adequate focus and resolution. In Figs. 3(d) and 3(d′) the structure is seen finally to become fully parallel-plate-like. The plate width increases between Figs. 3(b),(b′) and 3(d),(d′). It can be observed from micrographs taken in normal light that the β-equiaxed primary grain size grows in the same direction.

The weld zone structures are the following:

In the tube's heat-affected zone [Figs. 5(a) and 5(a′)] the original textured structure (Fig. 2) is transformed into α-equiaxed grains.

There follows [Figs. 5(b) and 5(b′)] a fine acicular structure (Wbα).

Near the fusion zone the structure is Wbα with a certain proportion of Wppα [Fig. 5(c)]. In Fig. 5(c′) the preexisting β grain boundaries are clearly delineated.

At the fusion zone the structure is predominantly Wppα with islands of Wbα [Fig. 5(d)]. The β primary grains are larger [Fig. 5(d′)].

The end-cap structure is fully Widmanstätten (Fig. 6). It changes from

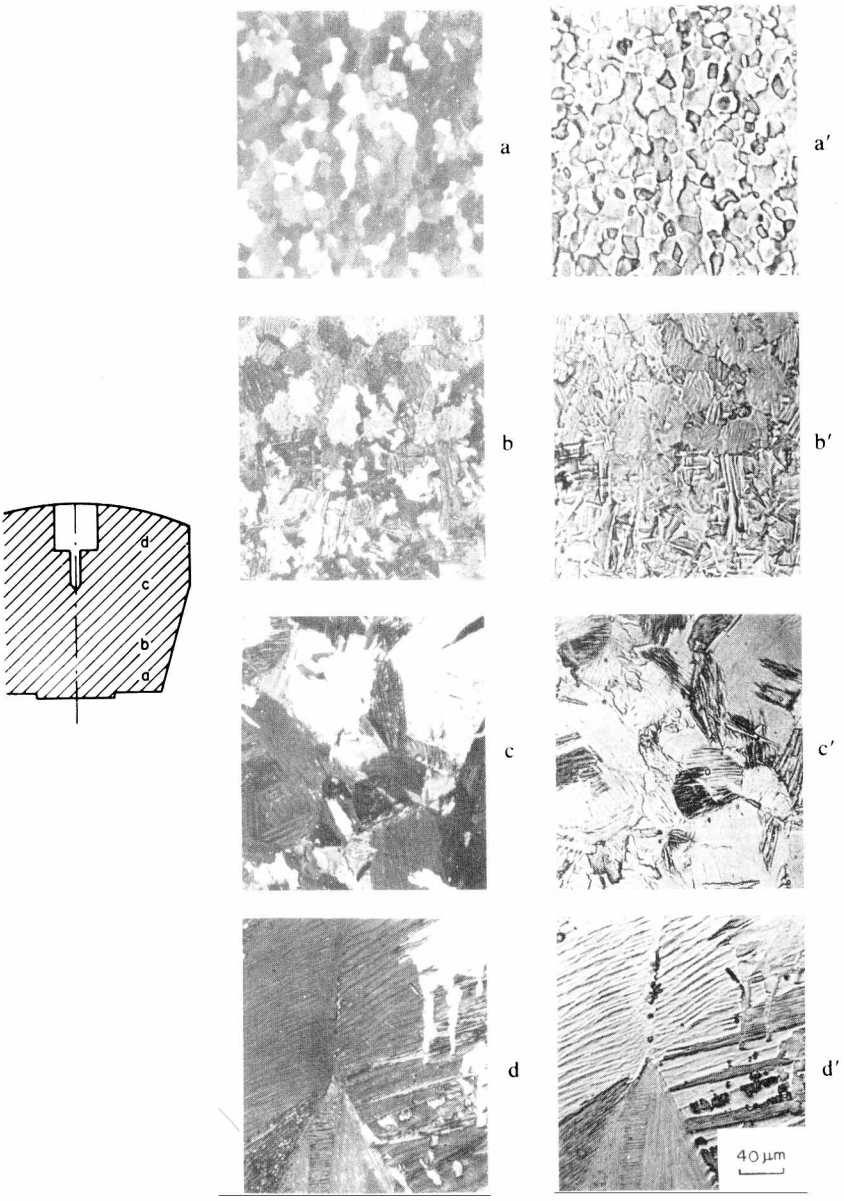

FIG. 3. End-cap structure before welding, showing optical micrographs taken in polarized [(a)–(d)] and normal [(a′)–(d′)] light.

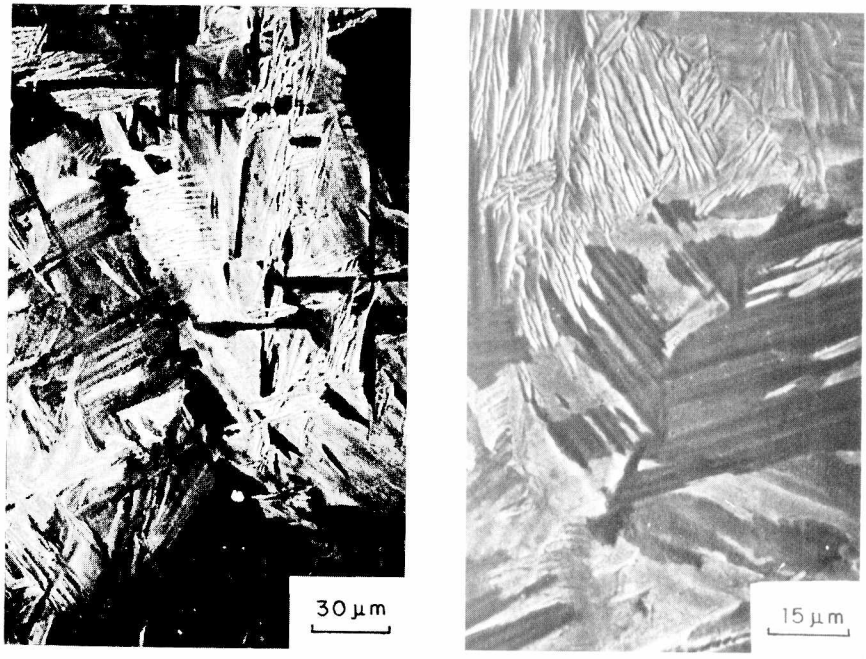

FIG. 4. Scanning electron micrographs of the end cap before welding, showing the basketweave zone.

parallel-plate Wppα [Fig. 6(a)] to an intermediate type with varying proportions of Wppα and Wbα [Fig. 6(b)].

The originally equiaxed zone [Figs. 3(a) and 3(a′)] changes into a fine basketweave structure [Fig. 6(c)]. The difference in primary β grain size, previously observed in Fig. 3, is emphasized after welding.

Discussion

The structures obtained after welding are the result of the interaction of the thermal cycle associated with the process involved and the characteristics of the material (such as chemical composition and previous thermomechanical treatment). The effect of the thermal cycle is a function of the maximum temperature reached, the time at high temperature (>1000°C for Zircaloy), and the cooling rate (from 1000°C for Zircaloy). The structures obtained must be analyzed with these factors taken into account.

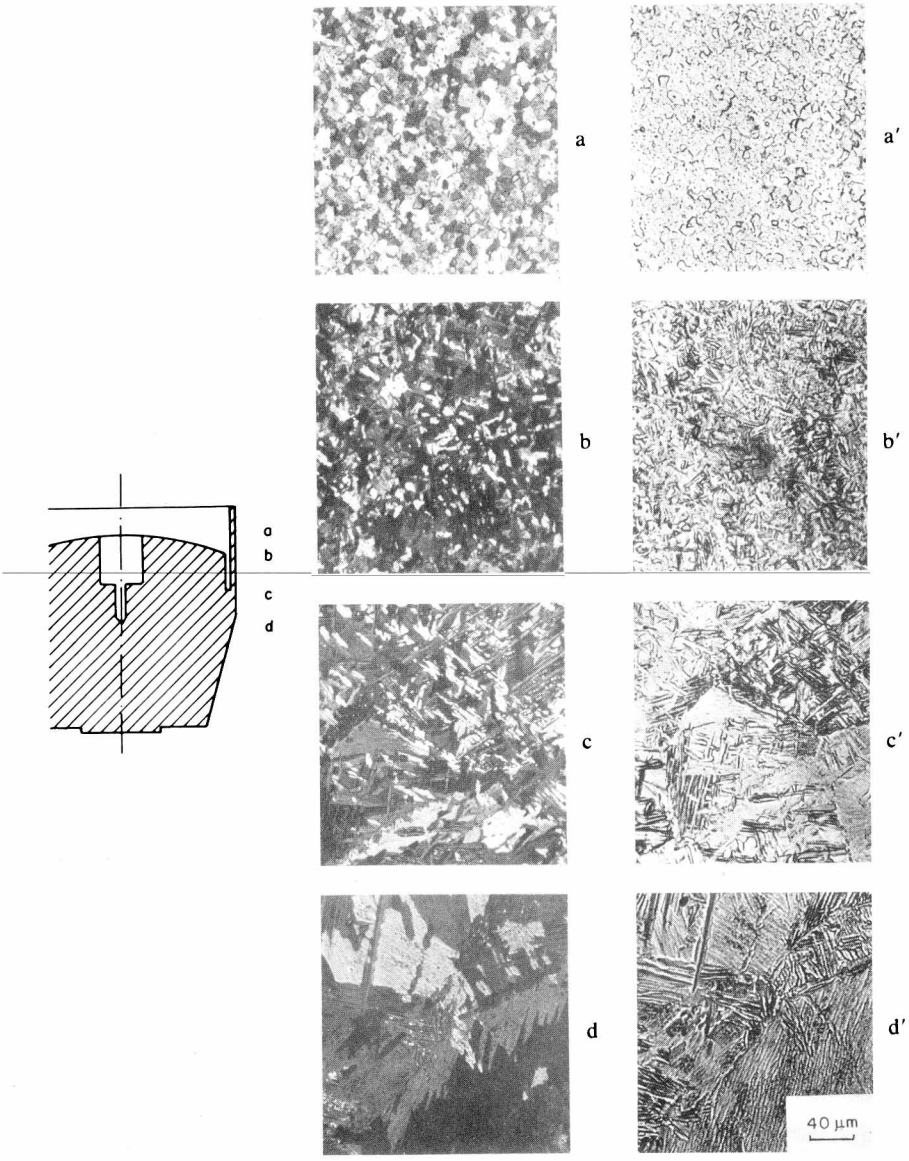

FIG. 5. Welding structure, showing optical micrographs taken in polarized [(a)–(d)] and normal [(a')–(d')] light.

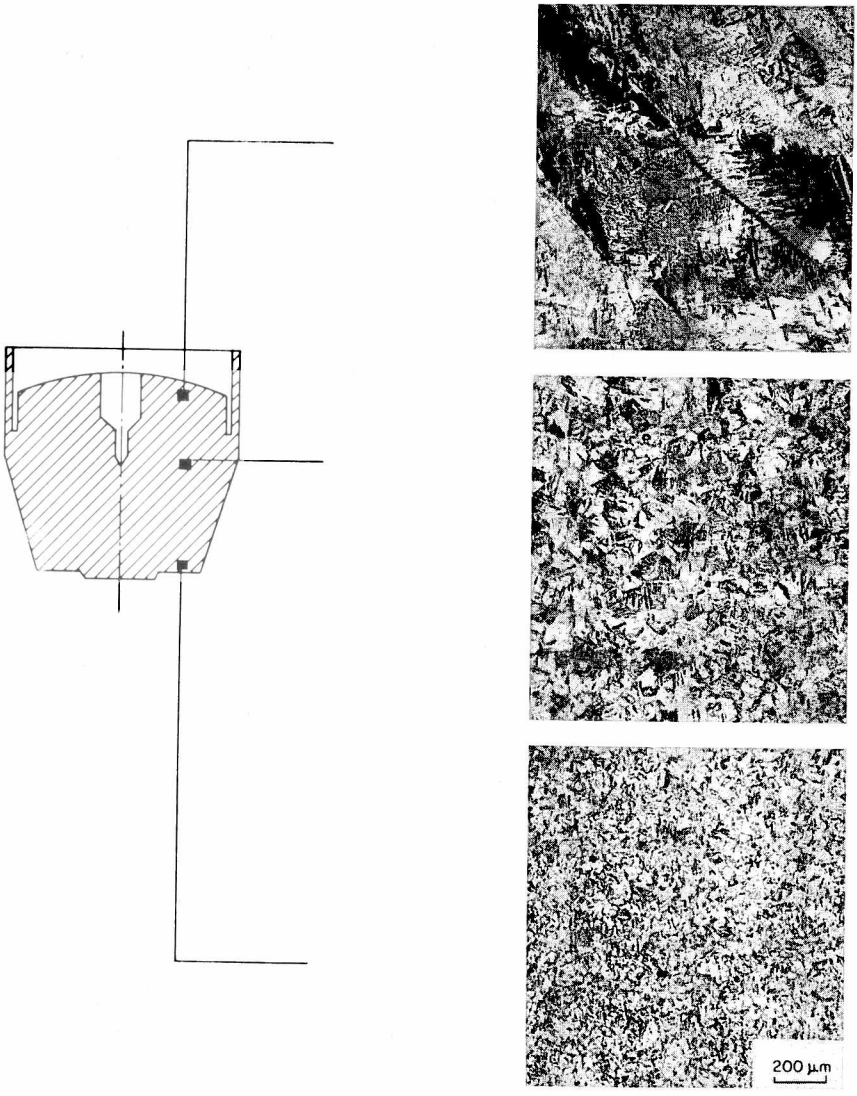

FIG. 6. End-cap structure after welding, showing optical micrographs taken in polarized [(a)–(d)] and normal [(a′)–(d′)] light.

The tube originally had a highly deformed structure (Fig. 2); this recrystalized and grew in α phase as equiaxed grains [Figs. 5(a) and 5(a′)]. In the subsequent regions, the β primary grain size increases, as is shown in Figs. 5(b′)–5(d′). This growth occurs because these regions reached the β phase and were at temperatures higher than 1000°C [4] for increasing

TABLE 1
Correlation of Cooling Rate with the β→α Transformation Structure of Zircaloy-4

Cooling rate (C°/sec)	Microstructure type
≳1500	martensitic
1500–600	intermediate martensitic–basketweave
600–10	basketweave
10–2	intermediate basketweave–parallel-plate
2–0.5	parallel-plate
≲0.5	lenticular

periods of time. The associated secondary structures [Figs. 5(b)–5(d)] change from very fine Wbα type to a coarse Wppα structure of parallel plates, with an intermediate zone of Wbα + Wppα. According to Table 1 [4], this is caused by a change in the cooling rates between 600 and 10 C°/sec. The cooling rate was higher in the tube, where the heat transfer is through the unheated part. On the other hand, in the fusion zone the whole end cap reached temperatures high enough to diminish the heat extraction by several orders of magnitude.

Because the end caps are heated nonuniformly before welding, the structure at the location shown for Fig. 6(a) is of large β primary grains. Far from the heat source, the time in β phase ($T > 1000$°C) decreases, and consequently the antecedent β grain size diminishes [from Fig. 3(d′) to Fig. 3(b′)]. At the same time, the cooling rate increases and (see Table 1) the secondary structure changes from coarse parallel plate (Wppα), through fine basketweave (Wbα), to martensitic colonies of Mα′ (at a cooling rate in excess of 1500 C°/sec; see Table 1). At the top of the end cap a zone that remained in the α phase is observed [Figs. 3(a) and 3(a′)].

During welding the whole end cap reached the β phase. Then the secondary structure shows a gradual change from a coarse Wppα structure in the fusion zone to a fine Wbα structure at the top of the end cap. The primary grain size decreases from the fusion zone to the top, and in each zone the sizes are larger after welding.

Summary

In gas tungsten arc welds of end caps to tubes the joint suffers a variation of thermal cycles with cooling rates over the range $10–10^3$ C°/sec.

For this reason a variety of microstructures with very different properties are present after welding:

a. At the fusion zone (cooling rate of 2–10 C°/sec) the secondary structure is coarse Wppα.
b. From the fusion zone and along the tube, the cooling rates change from 10 to 10^3 C°/sec with the sequence of structures

$$\text{Wpp}\alpha \rightarrow \text{Wpp}\alpha + \text{Wb}\alpha$$
$$\rightarrow \text{Wb}\alpha \text{ (with fine plates).}$$

c. In the remote heat-affected zone the α phase recrystalizes and small polygonal grains are obtained.
d. From the fusion zone to the top of the end cap, the structures are

$$\text{Wpp}\alpha \rightarrow \text{Wpp}\alpha + \text{Wb}\alpha$$
$$\rightarrow \text{Wb}\alpha.$$

The authors gratefully acknowledge the financial support of the Welding Technology Project SECYT-CNEA.

References

1. O. Woo and K. Tangri, Transformation characteristics of rapidly heated and quenched Zircaloy-4 oxygen alloys, *J. Nucl. Mater.* 79:82–94 (1979).
2. G. Ökvist and K. Källström, The effect of Zirconium carbide on the β → α transformation structure in Zircaloy, *J. Nucl. Mater.* 35:316–321 (1970).
3. R. A. Holt, The beta to alpha phase transformation in Zircaloy-4, *J. Nucl. Mater.* 35:322–334 (1970).
4. H. M. Chung, A. M. Garde, and T. F. Kasner, Mechanical properties of Zircaloy containing oxygen, Light-Water Reactor Safety Research Program Quarterly Progress Report ANL 77-10, Section III (October–December 1976).

Received March 1981; accepted July 1981

COMISION NACIONAL DE ENERGIA ATOMICA
CENTRO DE INFORMACION C.A.C.